scientific reports

Check for updates

OPEN

Unidirectional propagation of the Bloch surface wave excited by the spinning magnetic dipole in two-dimensional photonic crystal slab

Li-Ming Zhao✉ & Yun-Song Zhou

The photonic spin Hall effect (PSHE) can be realized in a photonic crystal (PC) slab, that is, the unidirectional Bloch surface wave can propagate along the surface of the PC slab under the excitation of elliptical polarized magnetic dipole. It is further proved that PSHE is caused by the interference of the component surface waves excited by the different components of the incident light, which is the so called component wave interference (CWI) theory. In addition, we also find that the spin of the surface wave oscillates periodically in space, and the oscillation period is a unit cell. In a unit cell, the average spin keeps the spin orbit locked. The results show that the spin separation can also be modulated by the position and the polarization state of the magnetic dipole.

Photonic spin Hall effect (PSHE) can separate photons according to different spin characteristics, which provides a new idea for the design of photonic devices and has important application prospects[1–8]. In 2013, Zayats et al. observed a new kind of PSHE in metal system, and found that surface plasmon polariton (SPP) can propagate unidirectionally, and the propagation direction can be controlled by the incidence of circularly polarized light[9]. Different from the traditional PSHE, the new PSHE has a strong Hall effect, which obviously separates the beams with different spin. The main explanations about PSHE are wavevector matching (WVM)[10,11] and spin coupling theories[12]. For SPP, its spin is a transverse angular momentum, which has a chirality relationship with the surface and transmission direction. This chirality is an invariant, commonly known as spin orbit locking[13–19]. According to the spin coupling theory, the incident spin determines the spin of SPP, and then the spin of SPP determines the propagation direction of SPP. Recently, it has been found that the asymmetric scattering of PSHE is caused the component wave interference (CWI) of electric or magnetic dipoles[20–22]. According to CWI theory, the propagation direction of SPP is determined by the incident spin, and then the spin of SPP is determined by the spin orbit locking of SPP.

The surface waves in photonic crystal (PC) are the Bloch surface waves composed of zero order and higher order surface modes. In recent years, PSHE can be observed in two-dimensional (2D) PC[23], and an open cavity was regarded as a scatterer. As we all know, an electric dipolar source or magnetic dipolar source can be realized experimentally by illuminating any small scatterer[10,24], therefore, the scattering of scatterer is equivalent to the radiation of the dipole source.

Based on the above works, we use a magnetic dipole source instead of the scatterer as a general theoretical model to study theoretically the following two issues: Whether the mechanism of generating PSHE by Bloch surface waves is similar to that of SPP? Can the spin orbit locking always be satisfied? It is found that the asymmetric scattering of PSHE of the Bloch surface wave results from the CWI theory, which is affected by the polarization and the position of the magnetic dipole. It is further found that there exists the locked relationship between average spin with orbit.

Department of Physics, Capital Normal University, Beijing 100048, China. ✉email: zlm-phy@cnu.edu.cn

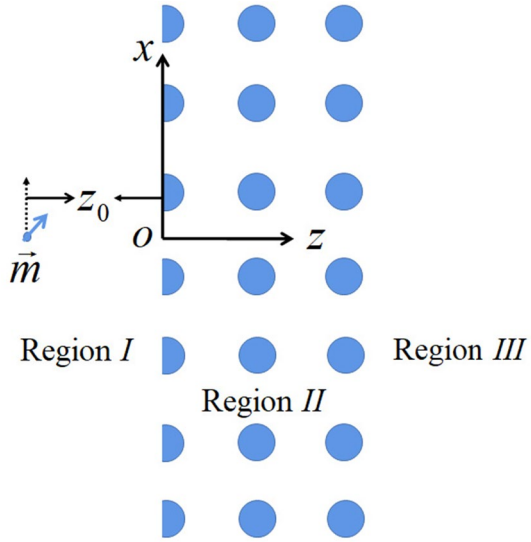

Figure 1. Sketch map of 2D PC slab, a magnetic dipole pillar $\vec{m}$ is located at $x = 0$ and $z = z_0$.

Radiation of magnetic dipole

The system investigated is a PC slab, it can divide the space into three regions, as shown in Fig. 1. The PC slab is located in region *II* and surrounded by air on either side (referred to regions I and III). The PC consists of a square lattice (with lattice constant a) of cylinders (with radius *r*). The periodic plane layers are laid on the xz plane and the cylinders are infinite along the y-direction, and the periodic layers along z-direction are finite, while along x-direction are infinite. In order to generate the interface states, the rods in the leftmost layer have been truncated along their diameter into a semicircular shape. In this paper, we just consider the E-polarized interface states, which can be excited by a magnetic dipole $\vec{m}$. Now, it is assumed that there is a magnetic dipole cylinder located in region *I* at $x = 0$ and $z = z_0$, and the interface between Region *I* and *II* is set as $z = 0$. The magnetic dipole can radiate the electromagnetic wave, and the corresponding magnetic vector potential can be written as

$$\vec{A}(x,z,\vec{m}) = \frac{i\mu_0}{4\pi}\int_{-\infty}^{\infty} dy(\vec{k}\times\vec{m})\frac{e^{ik|\vec{\rho}-y\hat{y}|}}{|\vec{\rho}-y\hat{y}|} = \frac{-\mu_0}{4\pi}\int_{-\infty}^{\infty}(\vec{k}\times\vec{m})\frac{dk_x}{k_z}e^{i(k_x x+k_z|z-z_0|)}, \tag{1}$$

here, $\vec{\rho} = x\hat{x} + (z - z_0)\hat{z}$, $\vec{m} = (m_x, 0, m_z)$, and $k_z = \sqrt{k^2 - k_x^2}$, where k is the wavenumber of the radiation field. According to Maxwell equation

$$\vec{H} = \frac{1}{\mu_0}\nabla\times\vec{A} = \frac{-1}{4\pi}\int_{-\infty}^{\infty}\frac{dk_x}{k_z}i\vec{k}\times(\vec{k}\times\vec{m})e^{i(k_x x+k_z(z-z_0))}.$$

Here, we just consider the region $z > z_0$, and considering $\vec{k} = (k_x, 0, k_z)$ and $\vec{k}\times(\vec{k}\times\vec{m}) = (k_x k_z m_z - k_z^2 m_x)\hat{x} + (k_x k_z m_x - k_x^2 m_z)\hat{z}$, $\vec{H}$ can be rewritten as

$$\vec{H} = \frac{-i}{4\pi}\int_{-\infty}^{\infty}\frac{dk_x}{k_z}[(k_x k_z m_z - k_z^2 m_x)\hat{x} + (k_x k_z m_x - k_x^2 m_z)\hat{z}]e^{i(k_x x+k_z(z-z_0))},$$

and the corresponding electric field is

$$\vec{E} = \frac{i}{\omega\epsilon_0}\nabla\times\vec{H} = \frac{ik^2}{4\pi\omega\epsilon_0}\int_{-\infty}^{\infty}\frac{dk_x}{k_z}(k_x m_z - k_z m_x)\hat{y}e^{i(k_x x+k_z(z-z_0))},$$

where ε_0 and μ_0 are permittivity and permeability of the air.

When the electromagnetic wave propagates at the interface of the PC slab, the corresponding incident field can be rewritten as

$$\vec{E} = \frac{ik^2}{4\pi\omega\epsilon_0}\sum_n\int_{-\pi}^{\pi}\frac{dk_x}{k_{nz}}[(k_x + nG_x)m_z - k_{nz}m_x)]e^{i[(k_x+nG_x)x+k_{nz}(z-z_0)]}\hat{y}. \tag{2}$$

here, k_x is the Bloch wave vector and it is in the first Brillouin Zone (FBZ), and correspondingly, the $n-th$ order incident coefficients is $A_1^n = \frac{1}{k_{nz}}[(k_x + nG_x)m_z - k_{nz}m_x)]e^{-ik_{nz}z_0}$. The corresponding reflection field can be written as

$$\vec{E}_r(x,z) = \frac{ik^2}{4\pi\omega\epsilon_0}\sum_n\int_{-\pi}^{\pi}dk_x B_1^n e^{i[(k_x+nG_x)x-k_{nz}z]}\hat{y}, \tag{3}$$

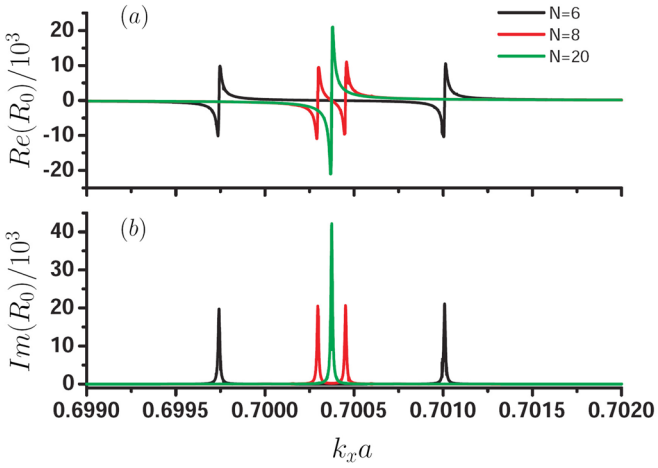

Figure 2. Reflection coefficients R_0 for $\omega = 0.3(2\pi c/a)$ as a function of k_x for different periodic layer number N of the PC slab, black curve for $N = 6$, red curve for $N = 8$, and green curve for $N = 20$, (**a**) is the real part of R_0, and (**b**) is the imaginary part of R_0.

here B_1^n can be obtained by Eq. (A6).

Now, we assume the surface wave $\vec{E}_{SW} = \vec{E}_r + \vec{E}_{pr}$, and $\vec{E}_{pr}$ is the radiation field and $\vec{E}_{pr} = \frac{ik^2}{4\pi\omega\epsilon_0}\sum_n \int_{-\pi}^{\pi} dk_x A_1^n e^{i[(k_x+nG_x)x-k_{nz}z]}\hat{y}$. Thus, the surface wave is

$$\vec{E}_{SW} = \frac{ik^2}{4\pi\omega\epsilon_0}\sum_n \int_{-\pi}^{\pi} dk_x (A_1^n + B_1^n) e^{i[(k_x+nG_x)x-k_{nz}z]}\hat{y}. \tag{4}$$

Once $\vec{E}_{SW}$ is known, the power of the surface wave in Region I is

$$\bar{P} = \int_{-\infty}^{0} dz 0.5 Re\left(\frac{1}{i\mu_0\omega} E_{SW}^* \frac{\partial E_{SW}}{\partial x}\right), \tag{5}$$

and the corresponding spin angular momentum density of surface wave can be written as[25,26]

$$\vec{S} = \frac{1}{4\omega} Im(\vec{D}_{SW}^* \times \vec{E}_{SW} + \vec{B}_{SW}^* \times \vec{H}_{SW}). \tag{6}$$

For E-polarized field, Eq. (6) can be rewritten as

$$\vec{S} = \frac{1}{4\omega} Im(\vec{B}_{SW}^* \times \vec{H}_{SW}), \tag{7}$$

and the corresponding energy density of the surface wave is

$$W = \frac{1}{4}\mu_0 |H_{SW}|^2. \tag{8}$$

According to Eqs. (7) and (8), we can obtain the average spin for one photon is

$$\bar{s} = \frac{Im(\vec{H}^* \times \vec{H})}{|H|^2}\hbar. \tag{9}$$

Results and analysis

We assume that the two-dimensional PC is composed of a square lattice of dielectric cylinder with a dielectric constant 11.56 and radius $r = 0.2a$. We have calculated the band structure by using the plan-wave expansion method and found that the photonic band gap (PBG) of E-polarized field is located in the circular frequency range of $0.286 - 0.42(2\pi c/a)$. In Fig. 2, we first investigate the reflection coefficients R_0 (It can be obtained by Eq. (A9)) as a function of k_x for different period layer number N of the finite PC slab when $\omega = 0.3(2\pi c/a)$, black curve for $N = 6$, red curve for $N = 8$, and green curve for $N = 20$. Due to R_0 is a complex number, the variation of real part of R_0 denoted by $Re(R_0)$ with k_x is presented in Fig. 2a and the variation of imaginary part of R_0 denoted by $Im(R_0)$ with k_x is shown in Fig. 2b. It is noting that the reflection wave is the superposition of n plan waves, the corresponding wave vectors along x direction are $k_x + mG_x$, here $m = -n/2, -n/2+1, ...0, 1, ...n/2$. Therefore, there are n corresponding reflection coefficients. The calculation results show that the $0-th$ reflection coefficient is the largest, for the higher-order reflection coefficients, their values are decreases rapidly. Moreover, the variation curves of other higher-order reflection coefficients with k_x are similar with that of the $0-th$ reflection coefficient, so we only give the variation of $0-th$ reflection coefficient R_0 with k_x in Fig. 2. It

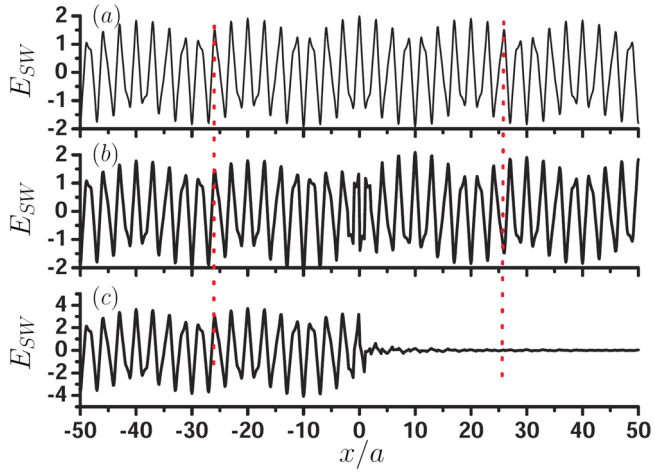

Figure 3. Surface field at $z = 0$ as a function of x for different $\vec{m}$, (**a**) for $\vec{m} = cos58^\circ e^{-i\omega t}\hat{x}$, (**b**) for $\vec{m} = isin58^\circ e^{-i\omega t}\hat{z}$, and (**c**) for $\vec{m} = (cos58^\circ\hat{x} + isin58^\circ\hat{z})e^{-i\omega t}$.

should be emphasized that the curve R_0 with k_x is symmetrically distributed with respect to $k_x = 0$. It is found that there are two singular points for the reflection coefficients in the case of $N = 6$ and $N = 8$, for $N = 6$, the singular point are $k_x a = 0.69975$ and 0.70101, and for $N = 8$, the corresponding singular points are 0.7003 and 0.70045. We further found that with the increase of N, the distance of the two singular points are smaller, and when $N = 20$, the singular point is about $k_x a = 0.70038$ and the curve of the reflection coefficient is similar to that of SPP, and the singular point is corresponding to the interface modes. We also obtain the interface modes for other frequencies by the singular behavior of the reflection coefficient, and finally, we find that our results are similar with Fig. 4 in Ref.[27]. It is worth noting that the reflection coefficient can also be regarded as the excitation rate of the surface state, when its absolute value is larger, the ability to excite surface states is stronger.

Now, we investigate the asymmetric scattering (unidirectional scattering) of PSHE for the above PC slab in the case of $N = 6$. For simplicity, let's assume that a magnetic dipole $\vec{m} = (cos\theta\hat{x} + isin\theta\hat{z})e^{-i\omega t}$ illuminates the system, and θ is polarization angle, the position of $\vec{m}$ is set as $z_0 = -0.1a$. Figure 3 shows the field at the interface (arbitrary unit (A. U)) as a function of x for different $\vec{m}$, (a) for $\vec{m} = cos58^\circ e^{-i\omega t}\hat{x}$, (b) for $\vec{m} = isin58^\circ e^{-i\omega t}\hat{z}$, and (c) for $\vec{m} = (cos58^\circ\hat{x} + isin58^\circ\hat{z})e^{-i\omega t}$, here $\omega = 0.3(2\pi c/a)$. As can be seen from Fig. 3a, the surface field excited by m_x is the even function of $x = 0$, and the surface field excited by m_z is a odd function of $x = 0$, as shown in Fig. 3b. For the curve in Fig. 3c, it comes from the superposition of the curves in Fig. 3a,b, obviously, this curve presents an asymmetric behaviors. There are two vertical red dashed lines through the three graphs in Fig. 3, the left one shows that the two component waves (Fig. 3a,b) in $x < 0$ region are instructive interference, so the total wave propagating to the left is strong. Similarly, the right one are interference destructively, so the total wave (Fig. 3c) propagating to the right is suppressed. In other words, the asymmetric scattering results from the superposition of fields with different parity excited by two different components of magnetic dipoles, which is so-called CWI principle.

We can also see that the surface field in Fig. 3 shows some periodicity, and the period is about $20a$. It can be seen from Eq. (4) that the surface field is the superposition of Bloch waves with different Bloch wave vectors k_x. The larger the reflection coefficient, the greater the contribution to the surface field. According to Fig. 1, the Bloch waves of $k_x a = \pm 0.7\pi$ have the largest contribution on the surface field, and the superposition of the two component fields of $k_x x = \pm 0.7\pi$ can get $cos0.7\pi a$. In addition, due to the spatial periodicity of PCs, the period should be an integral multiple of the lattice constant. Therefore, we can finally obtain the corresponding period of the surface field is $\frac{7\times 2\pi}{0.7\pi} a = 20a$. We also calculate the surface field for $\omega = 0.315(2\pi c/a)$, when $k_x a = \pm 0.8\pi$, the reflection coefficient is the largest, and we finally find that the period of the corresponding surface field is $\frac{2\times 2\pi}{0.8\pi} a = 5a$.

Now, we study the spin properties of the surface wave in the region of $x < 0$, and the parameters are the same as those in Fig. 3c. The average spin of one photon of the surface wave can be obtained by Eq. (9). Figure 4 shows the variation of average spin $\bar{s}$ with x, it can be seen that the spin oscillates with a period of lattice constant a, which is different from the spin of the SPP, it is a constant and independent of position. It can be observed that in most regions (from -0.34a to 0.34a in a cell), the spin is less than 0 and has a large absolute value. Obviously, when $x < 0$, the average spin in the periodic unit is always less than 0, which means that the average spin and orbit are locked.

Now, we define the spin separation, it can be defined as $\eta = \frac{\bar{P}_+}{\bar{P}_+ + |\bar{P}_-|}$, here, $\bar{P}$ is the average power in a lattice, and $\bar{P}_+$ is the average power for $x > 0$, and $\bar{P}_-$ is the average power for $x < 0$. Therefore, when $\eta < 0.5$, the surface wave mainly travels to $x < 0$ direction, and $\eta > 0.5$, surface wave mainly propagates to right. In fact, the power oscillates periodically, and the oscillation period is the lattice constant a, which is an amazing result because power should be a constant. This can be understood because the energy of the surface field in the air and the surface field in the PC slab is mutually converted, therefore, the total energy is still conserved. In a

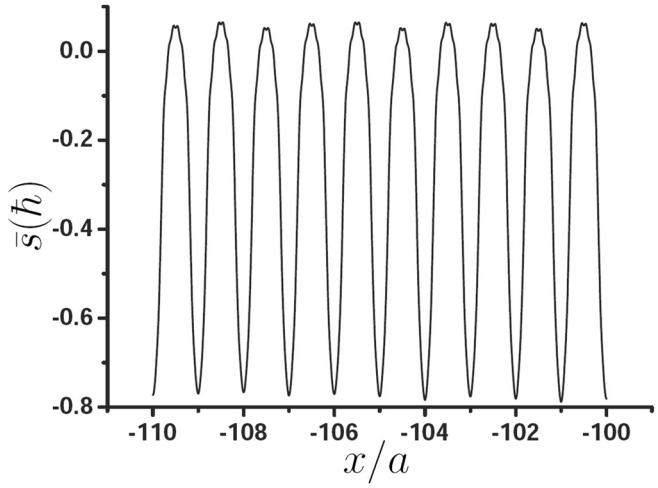

Figure 4. Variation of average spin $\bar{s}$ with x.

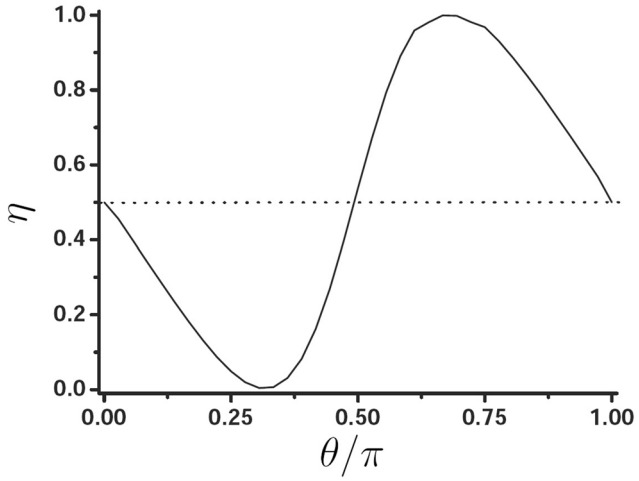

Figure 5. Spin separation as a function of polarization angle θ.

two-dimensional PC, the power oscillates with a period of a and the peak value of the power in the air corresponds to the valley value of the power in the PC. Finally, we obtain the spin separation is $\eta = 0.003$ for the parameters used in Fig. 3c.

Figure 5 presents the spin separation as a function of polarization angle θ. We find that when $\theta = 58°$ and 115°, the spin separation is the optimal, this denotes the optimal PSHE is an elliptically polarized light, not a circularly polarized light. We also calculate the variation of spin separation as a function of θ for $N = 20$, we finally find the optimal spin separation is the same with the case of $N = 6$, this indicates that the number of layer has little effect on the PSHE of surface wave.

Now, we discuss the influence of the magnetic dipole position z_0 on PSHE. Figure 6 shows that in the case of the optimal PSHE, θ and the corresponding η vary with $-z_0$. It can be seen that with the increase of the distance between the source with the interface, the optimal θ is decreased and the corresponding the spin separation is increased. That is to say, the smaller the distance between $\vec{m}$ and interface is, the better the PSHE is, this because with the decrease of the distance between the dipole and the interface, the corresponding interface field strength becomes stronger.

Summary

The mechanism of asymmetric scattering of PSHE in PC slab is investigated, and we find that it is caused by the interference of the component surface waves excited by the different components of the incident light. Different from the SPP, the average spin with the orbit is locked for the surface field in PC slab. In addition, we found that the spin separation degree depends strongly on the polarization and position of the magnetic dipole, but the layer of the slab has little effect on the PSHE.

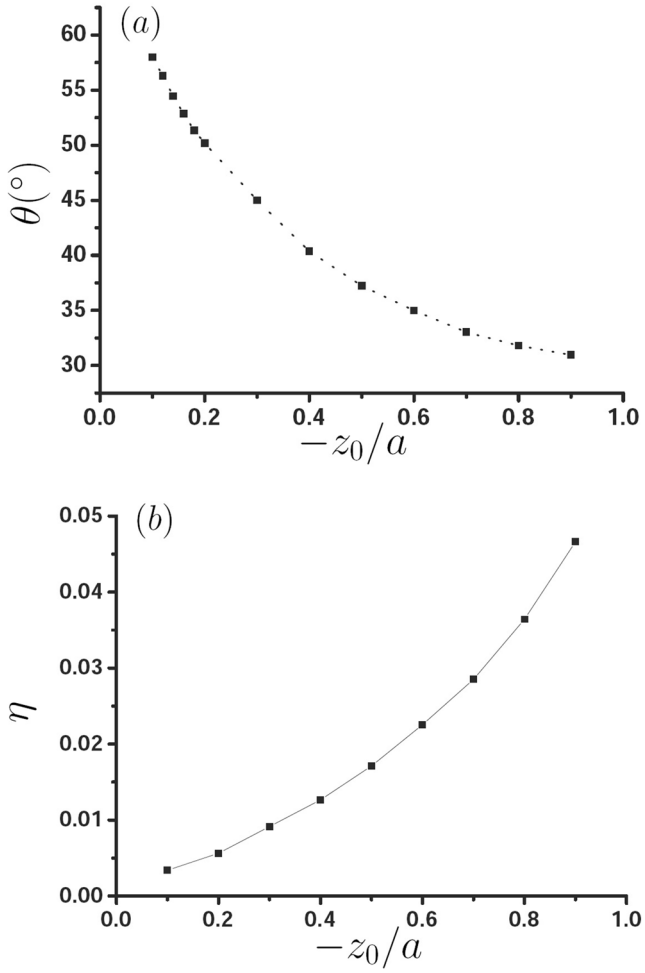

Figure 6. (**a**) Variation of the optimal θ with $-z_0$, (**b**) the optimal spin separation as a function of $-z_0$.

Received: 3 June 2021; Accepted: 26 July 2021
Published online: 16 September 2021

References

1. Imbert, C. Calculation and experimental proof of the transverse shift induced by total internal reflection of a circularly polarized light beam. *Phys. Rev. D* **5**, 787 (1972).
2. Bliokh, K. Y. & Aiello, A. Goos-Hanchen and Imbert-Fedorov beam shifts: An overview. *J. Opt.* **15**, 014001 (2013).
3. Jia, G. Y., Huang, Z. X., Ma, Q. Y. & Li, G. Photonic spin Hall effect on the surfaces of type-I and type-II Weyl semimetals. *Nanophotonics* **9**, 715 (2020).
4. Ling, X. H. *et al.* Revisiting the anomalous spin-Hall effect of light near the Brewster angle. *Phys. Rev. A* **103**, 033515 (2021).
5. Wang, Y. S., Chen, S. Z., Wen, S. C. & Luo, H. L. Realization of ultra-small stress birefringence detection with weak-value amplification technique. *Appl. Phys. Lett.* **118**, 161104 (2021).
6. Jia, G. Y., Zhang, R. X., Huang, Z. X., Ma, Q. Y. & Wang, H. W. Tunable photonic spin Hall effect due to the chiral Hall effect in strained Weyl semimetals. *New J. Phys.* **23**(7), 073010. https://doi.org/10.1088/1367-2630/ac068d (2021).
7. He, S. S. *et al.* Spatial differential operation and edge detection based on the geometric spin Hall effect of light. *Opt. Lett.* **45**, 877 (2020).
8. He, S. S. *et al.* Wavelength-independent optical fully differential operation based on the spin-orbit interaction of light. *APL Photonics* **5**, 036105 (2020).
9. Rodriguez-Fortuno, F. J. *et al.* Near-field interference for the unidirectional excitation of electromagnetic guided modes. *Science* **340**, 328 (2013).
10. Neugebauer, M., Bauer, T., Banzer, P. & Leuchs, G. Polarization tailored light driven directional optical nanobeacon. *Nano Lett.* **14**, 2546–2551 (2014).
11. Maier, S. A. *Plasmonics: Fundamentals and Applications* (Springer, 2007).
12. Bliokh, K. Y., Smirnova, D. & Nori, F. Quantum spin Hall effect of light. *Science* **348**, 1448 (2015).
13. Petersen, J., Volz, J. & Rauschenbeutel, A. Chiral nanophotonic waveguide interface based on spin-orbit interaction of light. *Science* **346**, 67–71 (2014).
14. O'Connor, D., Ginzburg, P., Rodriguez-Fortuno, F. J., Wurtz, G. A. & Zayats, A. V. Spin-orbit coupling in surface plasmon scattering by nanostructures. *Nat. Commun.* **5**, 5327 (2014).
15. le Feber, B., Rotenberg, N. & Kuipers, L. Nanophotonic control of circular dipole emission. *Nat. Commun.* **6**, 6695 (2015).
16. Bliokh, K. Y., Rodriguez-Fortunno, F. J., Bekshaev, A. Y., Kivshar, Y. S. & Nori, F. Electric-current-induced unidirectional propagation of surface plasmon-polaritons. *Opt. Lett.* **43**, 963 (2018).

17. Piao, X., Sunkyu, Yu. & Park, N. Design of transverse spinning of light with globally unique handedness. *Phys. Rev. Lett.* **120**, 203901 (2018).
18. Neugebauer, M., Eismann, J. S., Bauer, T. & Banzer, P. Magnetic and electric transverse spin density of spatially confined light. *Phys. Rev. X* **8**, 021042 (2018).
19. Bliokh, K. Y., Bekshaev, A. Y. & Nori, F. Optical momentum, spin, and angular momentum in dispersive media. *Phys. Rev. Lett.* **119**, 073901 (2017).
20. Picardi, M. F., Zayats, A. V. & Rodriguez-Fortuno, F. J. Janus and Huygens dipoles: Near-field directionality beyond spin-momentum locking. *Phys. Rev. Lett.* **120**, 117402 (2018).
21. Gao, Q., Zhou, Y. S. & Zhao, L. M. Continuous quantum photon Hall effect and its principle. *EPL* **133**, 27001 (2021).
22. Zhao, L. M. & Zhou, Y. S. Tunable multichannel Photonic spin Hall effect in metal-dielectric-metal waveguide. *Sci. Rep.* **11**, 14138 (2021).
23. Hu, J. B., Tian, S. N., Yang, Y. Z., Zhuang, S. L. & Guo, H. M. Dispersion engineering in unidirectional excitation of the surface wave of photonic crystal. *Opt. Lett.* **43**, 5319 (2018).
24. Evlyukhin, A. B. & Bozhevolnyi, S. I. Resonant unidirectional and elastic scattering of surface plasmon polaritons by high refractive index dielectric nanoparticles. *Phys. Rev. B* **92**, 245419 (2015).
25. Bliokh, K. Y., Dressel, J. & Nori, F. Conservation of the spin and orbital angular momenta in electromagnetism. *New J. Phys.* **16**, 09303 (2014).
26. Un, L. W. & Yen, T. J. Interface states and interface bulk correspondence of one-dimensional hyperbolic metamaterials. *Sci. Rep.* **7**, 43392 (2017).
27. Che, M. & Li, Z. Y. Analysis of surface modes in photonic crystals by a plane-wave transfer-matrix method. *J. Opt. Soc. Am. A* **25**, 2177 (2008).

Acknowledgements

This work was supported by the National Natural Science Foundation of China (NNSFC) under grant 11274233, 11004139, 21573079.

Author contributions

L.-M.Z. Obtaining PSHE in PC slab and Y.-S.Z. discussing the research content and checking and modifying the manuscript.

Competing interests

The authors declare no competing interests.

Additional information

Supplementary Information The online version contains supplementary material available at https://doi.org/10.1038/s41598-021-98056-y.

Correspondence and requests for materials should be addressed to L.-M.Z.

Reprints and permissions information is available at www.nature.com/reprints.

Publisher's note Springer Nature remains neutral with regard to jurisdictional claims in published maps and institutional affiliations.